Fused silica and silicon spring blades for the AEI prototype suspension

Madison Kaminskyj - Moravian College - University of Florida IREU
Host Advisors: Dr. Giles Hammond, Dr. Alan Cumming, and Mr. Karl Toland
kaminskyjm@moravian.edu

Institute for Gravitational Research, University of Glasgow - 31 July 2018

Abstract

The experiment measures the maximum deflection via testing silicon and fused silica spring blades on the spring breaking apparatus that was updated for this project. Then the values of fiber stress, maximum mass to be held, stiffness, and frequency of the various spring blades will be calculated for. There are five different sized silicon spring blades and three different shaped and surface fused silica spring blades that are being tested on this machine. The aim of this project is to figure out if fused silica or silicon can be used to replace the maraging steel spring blades specifically on the Suspension Prototype monolithic test suspension 100g masses, but for any suspension system in reality, in order to reduce the thermal noise caused by the metal. It is discovered that the correct parameters and shapes of either material can prove to be a promising start of a replacement of the metal spring blades in suspension systems.

I. Introduction

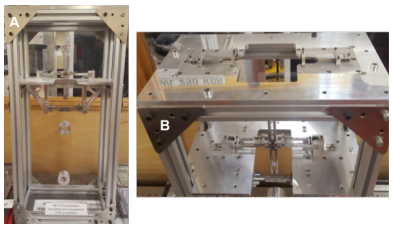

Figure 1: *Figure 1 image A shows the AEI 10m prototype monolithic test suspension (100g masses) at Glasgow. Image B shows the upper and lower spring blades that will be characterized and designed in silicon and fused silica in differing sizes.*

Albert Einstein predicted the existence of gravitational waves in 1914 through the theory he created called the Theory of General Relativity [1]. Einstein proposed that gravitational waves are ripples in space-time, which is a mathematical model that connects the three-dimension of space and one-dimension of time to a single four-dimensional continuum [2]. The proposition Einstein gave suggested that gravitational waves were results of large energetic processes. One example is black holes colliding [2]. In 2015 at Hanford, Washington and Livingston, Louisiana, the predictions set forth by Einstein were confirmed with the first detection of gravitational waves with the LIGO detectors [3]. It was through this discovery that his theory was confirmed and new opportunities in the gravitational waves field were opened.

The AEI 10 m prototype interferometer is set up at the AEI in Hannover Germany[4]. The AEI 10m prototype facility will be testing and developing advanced techniques that have the potential "for future upgrade the GEO-HF [including] digital control and data system, and high-power laser systems [as well as] provide training for scientists who will install these techniques in GEO-HF and operate that gravitational wave observatory" [4].

In this experiment the maraging steel spring blades

AEI 10m prototype monolithic test suspension (100g masses) at the University of Glasgow, shown in figure 1, were observed to model new spring blades made of different materials and varying sizes. The purpose of this was to reduce thermal noise that the metal spring blades cause as the wires in the prototype are copper, and the masses suspended at metal as well. The use of silicon or fused silica spring blades would improve the thermal noise not only in the AEI prototype, but these materials can also eventually replace metal spring blades in other experiments to cut down on noise. The main point of this project is to see if silicon or fused silica spring blades are useful materials in suspension systems.

Blade.jpeg

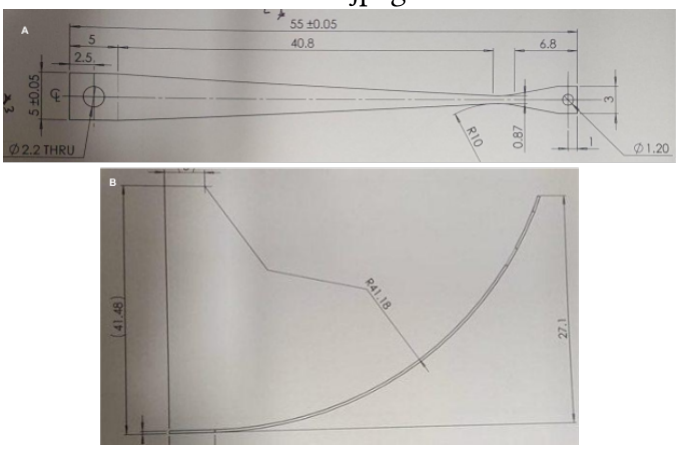

Figure 2: *Figure 2 This is the schematic drawing for the lower maraging steel spring blade currently in the AEI suspension prototype. (A) shows the aerial view of the blade and (B) shows the side view as the spring blade is curved. Each upper spring blade holds around 100 grams, both holding a total of 200 grams.The spring blades designed for this experiment made of silicon and fused silica will not be curved like this. The parameters of these blades are shown in the figure. This image comes from [5].*

The types of spring blades that are being tested are of different characteristics including size, shape, surface, and material. The spring blades that were designed for this experiment are made of fused silica and silicon and are based off of the current spring blades in the AEI Suspension Prototype monolithic test suspension 100g masses.

The spring blades in the AEI suspension are made of maraging steel. There are two different sized spring blades in the suspension system shown in figures 2 and 3.

Spring.jpeg

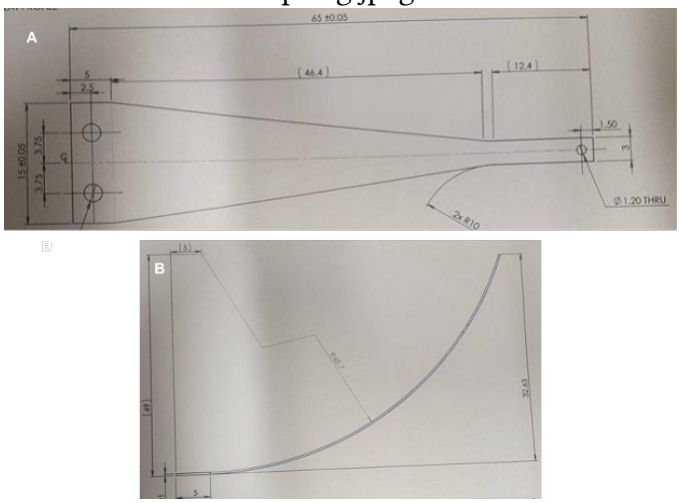

Figure 3: *Figure 3 This is the schematic drawing for the upper maraging steel spring blade currently in the AEI suspension prototype. (A) shows the aerial view of the blade and (B) shows the side view as the spring blade is curved. Each upper spring blade holds around 211.5 grams, both holding a total of 423 grams. The upper blades in the suspension system are larger than the lower suspension blades. The parameters of these blades are shown in the figure. This image comes from [6]*

There are predictive calculations for the maraging steel spring blades to check the equation for deflection that are shown in appendix A.

The fused silica spring blades had three different flavors that were tested. These included the untouched slide of fused silica glass which has a grounded surface (to be referred to as the square spring blade), a dremelled slide of fused silica to a similar shape of the metal blades to be referred to as the triangular spring blade, and lastly a flame polished version of the triangular slide to be referred to as the triangular flamed spring blade. A square flamed spring blade was made as well, but due to the inaccuracy of the flame polishing on the triangular spring blade it was decided to not make more and spend time else where.

vs dremel.jpeg

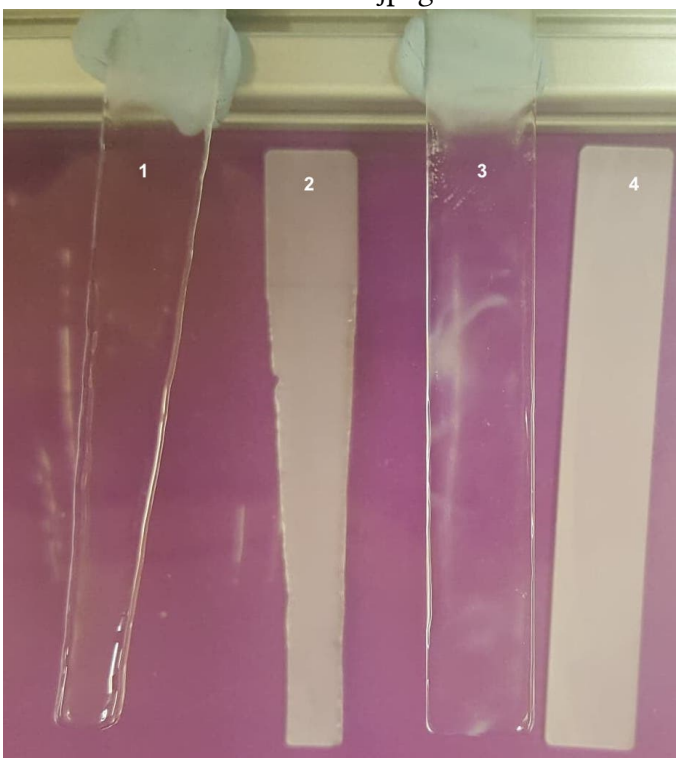

Figure 4: *Figure 4 shows the different flavors of fused silica slides observed. Slide one is the triangular flamed spring blade, the flame polishing sealed the ground cracks in the slide giving it a smooth and see through look. Slide two is the triangular spring blade that was dremelled to give the shape. Slide three is the square flamed spring blade which was not used for data for time's sake and due to the errors in the triangular flamed spring blade. Slide 4 is the unchanged square spring blade. The parameters for the three spring blades are shown in table 1*

Spring Blade	Width (mm)	Thickness (mm)	Length (mm)	Young's Modulus (GPa)
Triangular Silica	11.2	1.2	75.5	71.7
Square Silica	11.2	1.2	75.5	71.7
Silicon Blade 1	5	0.5	50	140
Silicon Blade 2	15	0.5	60	140
Silicon Blade 3	20	0.5	60	140
Silicon Blade 4	20	0.5	70	140
Silicon Blade 5	20	0.5	80	140

Table 1: *This table shows the parameters for every spring blade that is tested including the fused silica and the silicon spring blades. The young's modulus for silica comes from [11] and for silicon from [12].*

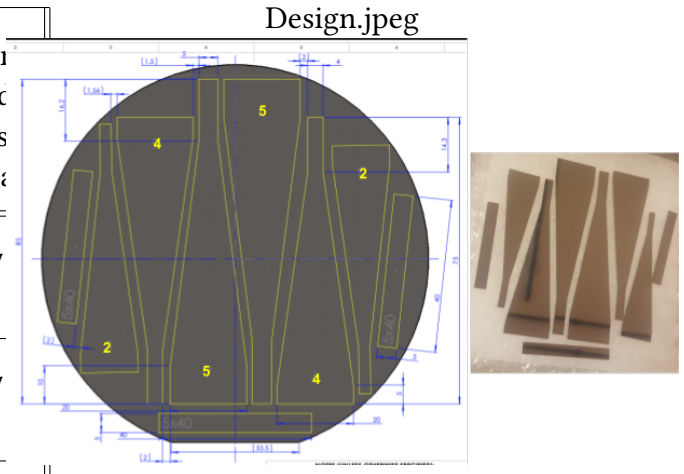

Figure 5: *Figure 5 is the first set of blade designs. The left image was sent to be laser cut and the right image is the final result of the silicon. There were three sets of this design cut from silicon wafers. It shows blade 2, 4, and 5. The CAD drawing comes from [7]*

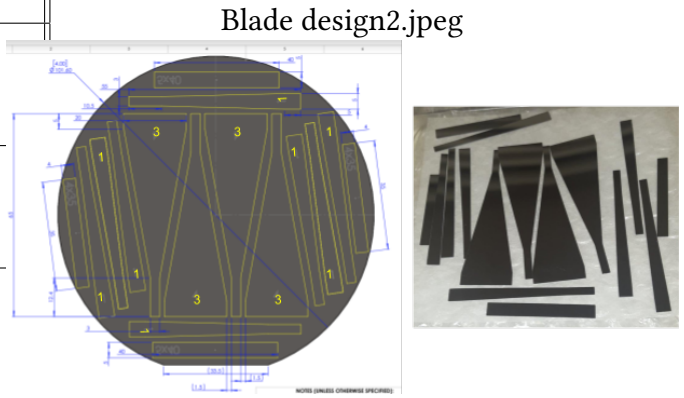

Figure 6: *Figure 6 is the second set of blade designs. The left image was sent to be laser cut and the right image is the final result of the silicon. There were two sets of this design cut from silicon wafers. It shows blades 1 and 3. The CAD drawing comes from [8]*

The other material that spring blades were designed from was silicon. The parameters for silicon is found in table 1. Sketches were made for the silicon spring blade designs and they are shown in appendix B. From these designs, a CAD drawing was made and then they were sent out to be laser cut. There were five different sized spring blades shown in figures 5 and 6 to be made out of the silicon with varying parameters that affected the deflection and fiber stress for each one differently.

With each different spring blade design there comes different issues. The surface of the square silica spring blade is ground and therefore the little surface imperfections that are uniform without tamper with the strength of the slide. It is the same issue for the triangular spring blade, but even more so because the sides are dremelled causing a loss in strength. The triangular

flamed spring blade was made to fix the surface imperfections, but because the flaming was not uniform and did not span the entire length of the spring blade, the strength was also negatively affected. The silicon spring blades surface is smooth and the edges were laser cut and uniform throughout each spring blade to the naked eye. In the future the edges will be examined under a microscope to see if there are imperfections and how uniform they truly are.

These spring blades will all be tested on the updated spring breaking apparatus to be discussed in the experimental model section. Throughout the project the spring breaking apparatus was fixed and updated for this specific experiment. There will also be a high speed camera used to capture the deflection of each spring blade and record data.

II. Experimental Model

For this experiment multiple different shapes and sizes, as well as two different materials of spring blades, were tested via a spring breaking apparatus that was updated during the course of the project. The original spring breaking apparatus was used in a breaking stress experiment for sapphire [9]. There were multiple changes that were made to it so that it better suited the spring blades being examined as well as upgrading it in general.

set up.png

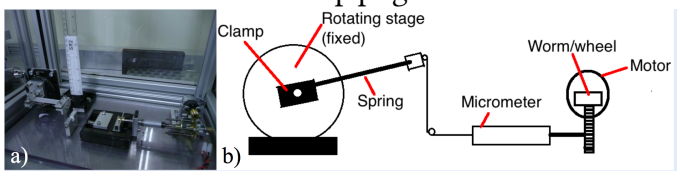

Figure 7: *Figure 7 was the original spring breaking apparatus for the breaking stress of sapphire experiment [9]. (a) shows the physical experimental set up, and (b) shows the diagram. This image came from [9].*

Figure 7 shows the apparatus was put together fully and setup properly. The starting point for this project began with parts of this apparatus broken, missing, or just needing an overall update.

SB machine.jpeg

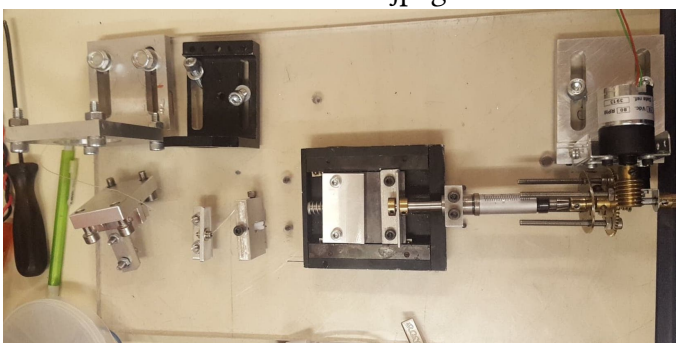

Figure 8: *Figure 8 shows what the apparatus looked like at the beginning of this project after not being in use for a while. One of the biggest issues with it was the gear and worm wheel connection. The teeth weren't meshing so the brass was being shaved off and broken down when the motor was running.*

new.jpeg

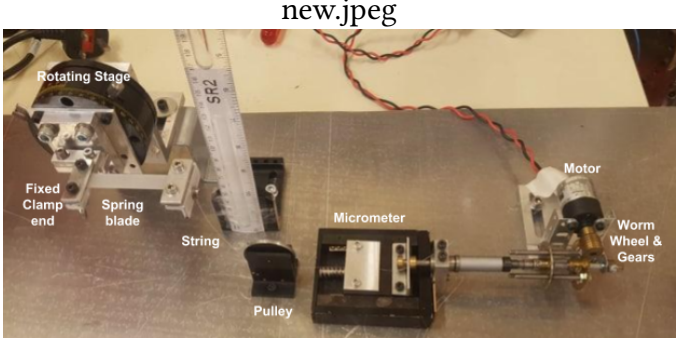

Figure 9: *Figure 9 is the current updated set up for the spring breaking apparatus. It is fully labelled showing the various parts of the setup.*

In figure 9 it is seen that there has been multiple updates to the original spring breaking apparatus. The way that the apparatus works was not changed but the overall function was improved and updated for this specific project. The base board was changes to steel for a sturdier foundation. The rotating stage was replaced and the cantilever spring blade clamp was attached to it. The pieces of metal that hold the spring blade in place on the clamp were replaced to match the size of the clamp. The pulley was replaced with the current one shown in figure 9 because the one before was impeding the string's pulling strength by

not having a circular rotation of the pulley. This pulley can also be moved closer to the rotating stage or further because of the different lengths of the spring blades.

The cantilever must be parallel to the pulley and the previously mentioned alteration made this possible for differing lengths. The micrometer jig needed to be elevated to be properly aligned with the motor, worm wheel, and gear combination. Previously there were screws that would raise it, but these screws hindered the plate the string was pulled by which caused strain on the gears. This was another reason for the brass shaving off of the gear/worm wheel as mentioned in the caption of figure 8.

Finally, the motor, worm wheel, and gear system needed to be realigned. I reconstructed the stand of the motor with Meccano parts and moved the gear so that it was centered and snug against the worm wheel to ensure it turned properly.

set up.jpeg

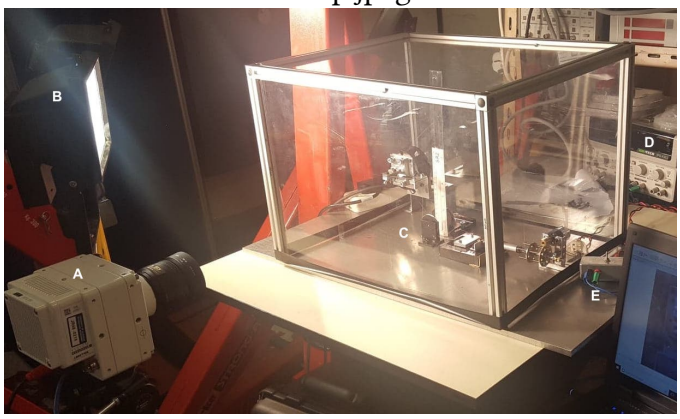

Figure 10: *Figure 10 shows the entire set up of the experiment. A is the Phantom high speed camera, B is the lighting fixture used for the camera, C is the box that surrounded the experiment to contain the shattering glass from the spring blades, D is the DC power supply used to power the motor, and E is the switch that turned the motor on and off and changed the direction of the worm wheel to push or pull the micrometer.*

Figure 9 shows how the apparatus works. The spring blade is clamped to the fixed end of the cantilever and the free end that's attached to the string. 12V is driven to the switch for the motor, the motor turns the worm wheel and gear combination to turn the micrometer. The switch can be flipped to either push or pull to change the direction of the micrometer. The micrometer slowly pulls the plate that the string is under. The string slowly pulls the spring blade down until the spring blade breaks. The moment of breaking is recorded by the high speed camera and then analyzed in slow motion. The starting point of the spring blade is subtracted from the point of maximum deflection, just before the spring blade breaks, which is observed from the video. After y, the deflection, is recorded the other values are calculated for and analyzed as shown in the Data/analysis section.

Specs.jpeg

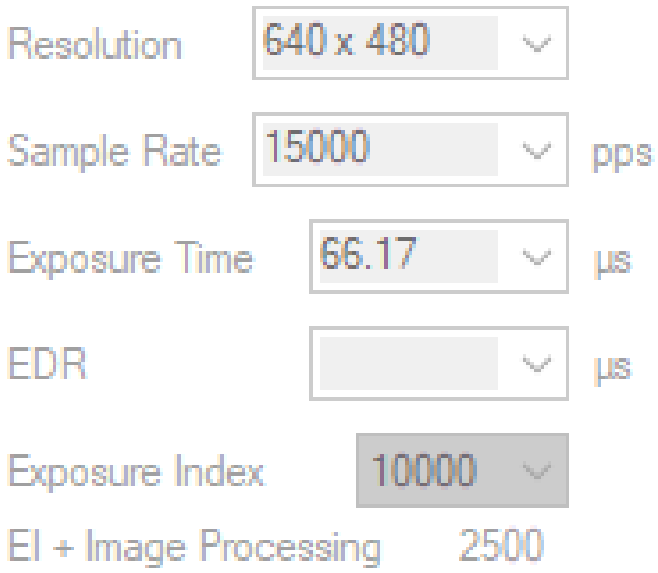

Figure 11: *Figure 11 shows the high speed camera specs.*

III. Mathematical Model

In the mathematical model the equations used for this experiment will be defined and derived. They will be used and shown in both the predictive calculated values in the introduction and the values calculated from experimental values found in the data and analysis section. The derivation in the mathematical model is from [10]:

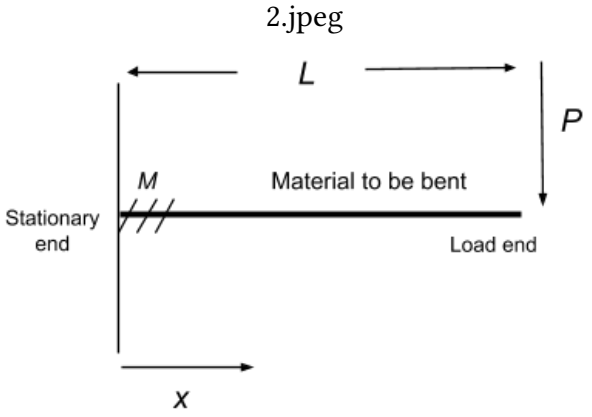

Figure 12: *The image above is a diagram of the bending moment on the curvature plane. The material to be bent (in this case a spring blade) is clamped to the stationary end and free on the load end for P, the vertical load, to act on it (in this case a string pulling on the spring blade). L is the length, x is the distance along the length that is being observed. The image is modelled after information in [13]*

Figure 12 is the pictorial version of the following bending moment equation:

$$M = P(L - x) \tag{1}$$

Where M is the bending moment, P is the vertical load, L is the Length, and x is the distance along the spring blade being observed.

'x' is wherever it is being observed because when x is 0, it is observed at the stationary end where the fiber stress is at its maximum value and deflection is at its minimum value, and when x is equal to L it is observed at the load end where the fiber stress is at its minimum value and deflection is at its maximum value. The equations for fiber stress and deflection will be derived below for both triangular and square spring blades.

Starting with the triangular spring blade calculations, the differential equation for the deflection is:

$$\frac{d^2y}{dx^2} = \frac{M_x}{EI} \tag{2}$$

Where E is young's modulus of the given material and I is the moment of inertia of the cross section about its neutral axis. âĂIJAlso, the product EI is known as the flexural rigidity that varies along the beamâĂİ [10]. We can substitute equation 1 into equation 2 for the following equation:

$$\frac{d^2y}{dx^2} = \frac{P(L - x)}{EI} \tag{3}$$

From here in order to solve for the deflection y we must substitute the equation for I shown:

$$I = (\frac{wt^3}{12})(\frac{L - x}{L}) \tag{4}$$

Where w is the width and t is the thickness. Equation 4 can be substituted into equation 3 for the following simplified equation:

$$\frac{d^2y}{dx^2} = \frac{12PL}{Ewt^3} \tag{5}$$

We can now integrate equation 5 twice to show the following equation for the deflection y:

$$y = \frac{6PLx^2}{Ewt^3} \tag{6}$$

The x^2 shows that the spring should indeed be curves like that of an arc of a circle. It should be noted that with the current maraging steel spring, the spring is curved so that when it is suspending a pendulum and weight it bends to have a bending moment of zero so that it is perfectly suspended. For this experiment silica and silicon cannot be bent first and then get back to a bending moment of zero like maraging steel. This is a problem with a solution to be discussed further in the conclusion.

It is also useful to show equation 6 solved for the vertical load P instead of y for it is how the data will be analyzed from recording the deflection and calculating the other values from it. The vertical load can be shown as:

$$P = \frac{y(Ewt^3)}{6Lx^2} \tag{7}$$

The fiber stress can be shown in the following equation:

$$\sigma = \frac{P(L - x)(\frac{t}{2})}{I} \tag{8}$$

Where σ is the fiber stress, and the thickness t is divided by two because the neutral zone in a spring is in the center so it is the distance from the to the stressed area. The fiber stress equation can be expanded by substituting equation 4 into equation 8 for the following equation:

$$\sigma = \frac{P(L-x)(\frac{t}{2})}{(\frac{wt^3}{12})(\frac{L-x}{L})} \tag{9}$$

Now the square spring blade equations can be defined. The differential equation for the deflection y is also integrated twice and simplified like the triangular equation. The derivation is began with equation 1 being substituted into equation 2. I in this case is different as the shape of the spring blade is different:

$$I = \frac{wt^3}{12} \tag{10}$$

Equation 10 is substituted into equation 3 for the following equation:

$$\frac{d^2y}{dx^2} = \frac{12P(L-x)}{Ewt^3} \tag{11}$$

To get the deflection y equation 11 is integrated twice and simplified for:

$$y = (\frac{12P}{Ewt^3})(\frac{-x^3}{6} + \frac{Lx^2}{2}) \tag{12}$$

It is useful again to solve equation 12 for the vertical load P shown as:

$$P = \frac{1}{\frac{12y}{Ewt^3}(\frac{-x^3}{6} + \frac{Lx^2/2}{2})} \tag{13}$$

The fiber stress for a square spring blade can be shown as:

$$\sigma = \frac{My}{I} \tag{14}$$

In equations 14, equations 1, 12, and 10 can be substituted and simplified for the following equation of fiber stress for square spring blades:

$$\sigma = \frac{P(L-x)(\frac{t}{2})}{wt^3} \tag{15}$$

Now the frequency, mass, and stiffness equations can be defined and they are the same for either square or triangular blades. The mass equation can be written as:

$$M = \frac{P}{g} \tag{16}$$

Where M is the mass, P is the vertical load, and g is gravity. The stiffness equation is:

$$k = \frac{P}{y_{max}} \tag{17}$$

Where k is the stiffness and y_{max} is the maximum deflection before breaking. Finally, we can define the frequency equation which has both the stiffness and mass in it:

$$f = \frac{\pi}{2}\sqrt{\frac{k}{M}} \tag{18}$$

Where f is the frequency.

IV. Data and Analysis

In the experiment the spring breaking apparatus broke various different sized silicon and fused silica spring blades of differing characteristics. In this section the individual data for each spring blade will be observed. The material of blade to be discussed first is the fused silica.

As mentioned in the introduction, there were three flavors of fused silica spring blade tested and the parameters are listed in the caption of table 1. The triangular flamed silica spring blades had very skewed results due to their configuration and unevenness of flame polishing. The individual and average data for the flamed triangular silica spring blades is in the appendix C. The triangular and square silica spring blade's deflection is shown in figure 14. The deflection was measured using the high speed camera which can be seen in figure 13.

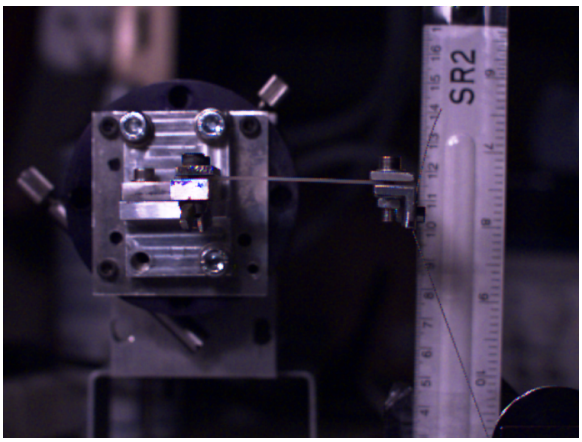

Figure 13: *Figure 13 shows the side view of the square silica spring blade from the high speed camera in front of the ruler used to measure deflection. The triangular silica spring blade also looks like this from the side angle.*

The triangular and square spring blade's fiber stress values are shown in figure 15. The results were constant as they followed suit with the deflection values, which the fiber stress was calculated from. The average results for both the fiber stress and deflection of each test will be shown in the analysis section.

Using equation 7 for the triangular spring blade values and equation 13 for the square silica spring blade, the deflection, and the variable's values corresponding with the spring blade, P, the vertical load can be solved for. P is the value needed to calculate the rest of the values to be analyzed so it must be solved for from the deflection. The results from calculating the vertical load, mass, frequency, and stiffness from recording the deflection for the silica spring blades, y, will be shown in the analysis section.

Figure 14: *Figure 14 shows the graph of the individual data collected from the high speed camera for the triangular and square fused silica spring bladesâĂŹ deflections. The blue bar is the square silica spring blade and the red is the triangular silica spring blade. Each test is listed on the horizontal axis and the vertical axis is the deflection of each spring blade test shown in meters. As the bar graph suggests the results were very constant. There is an error bar of reading the deflection from the high speed camera of + or - 0.5mm. There were a total of ten tests ran, therefore ten triangular and ten square silica spring blades were tested.*

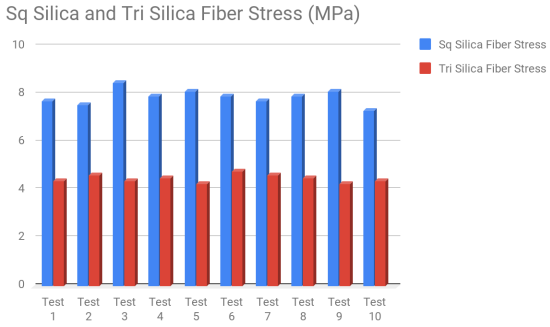

Figure 15: *Figure 15 shows the graph of the individual fiber stress values, calculated from the deflection that was collected from the high speed camera, for both the triangular and square fused silica spring bladesâĂŹ deflections. The blue bar is the square silica spring blade and the red is the triangular silica spring blade. Each test is listed on the horizontal axis and the vertical axis is the fiber stress of each spring blade test shown in MPa. As the bar graph suggests the results were very constant following suit with the deflection.*

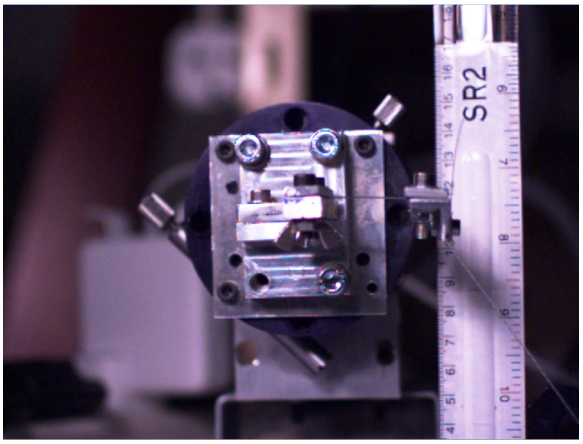

Figure 16: *Figure 16 shows the side view of the extra silicon spring blade from the high speed camera in front of the ruler used to measure deflection.*

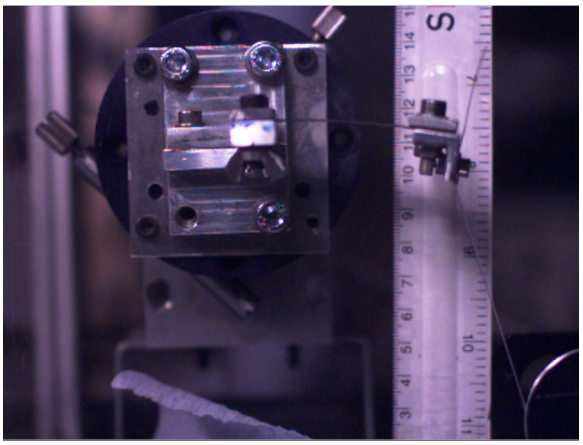

Figure 17: *Figure 17 shows the side view of silicon spring blade 4 from the high speed camera in front of the ruler used to measure deflection. Notice the bend in the silicon blade as a vertical load is being added to it. Once maximum deflection is hit the silicon spring blade will break.*

The silicon spring blade's deflection is shown in figure 18 and had relatively constant values in tests for each blade with both the deflection. The deflection was measured using the high speed camera and as shown in figure 17.

The silicon spring bladesâĂŹ fiber stress values are shown in figure 19. The results were constant as they followed suit with the deflection values, which the fiber stress was calculated from. The average results for both the fiber stress and deflection of each test of silicon spring blades will be shown in the analysis section.

Using equation 7 for the silicon spring blade values, the deflection, and the variable's values corresponding with the specific spring blade, the vertical load, P, can be solved for. The results from calculating the vertical load, mass, frequency, and stiffness from recording the deflection for silicon spring blades, y, will be shown in the analysis section.

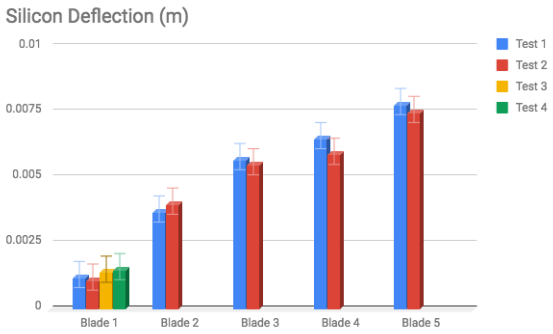

Figure 18: *Figure 18 shows the graph of the individual data collected from the high speed camera for the silicon spring bladesâĂŹ deflections. The differing colored bars were different tests ran for each of the five blades that are listed on the horizontal axis. The vertical axis is in meters. As the bar graph suggests the results were very constant in the tests for the spring blades. However, due to the supply of the specific numbered silicon spring blades only two-four tests could be run on each blade. Some need to be saved for future work listed in the conclusion. There is an error bar of reading the deflection from the high speed camera of + or - 0.5mm.*

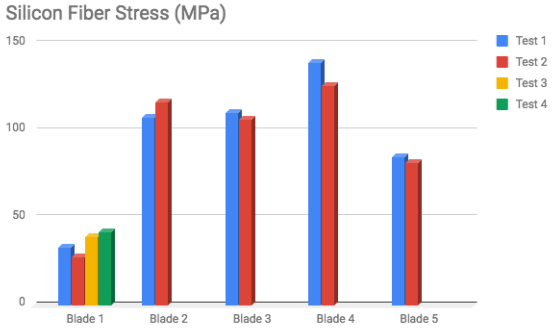

Figure 19: *Figure 19 shows the graph of the individual fiber stress values, calculated from the deflection that was collected from the high speed camera, for five different silicon spring bladesâĂŹ deflections. The differing colors in the bars distinct different tests. Each blade is listed on the horizontal axis and the vertical axis is the fiber stress of each spring blade test shown in MPa. As the bar graph suggests the results were very constant following suit with the deflection even though there are only two to four tests to compare for the blades.*

V. Analysis

In the experiment the spring blade breaking apparatus tested springs to obtain the deflection and then the fiber stress. It was also used to figure out how much mass each specific spring blade could hold, the frequency, and the stiffness of each spring blade. The average individual data for deflection and fiber stress for each of the types of spring blades will be shown in tables********** along with the stiffness and frequency. The deflection, y, was recorded from the high speed camera. The percent error, with recording the deflection off the high speed camera with the ruler has an error of $\pm 0.5mmandfortheplacementofspringbladesontheclampvaryingat \pm 3mm, was5.3\%.andtheandusedtocalculatetheverticalloadPusingequation7forthetriangularsilicaspringbladeandthe$

Spring Blade	x (mm)	y (mm)	P (N)	σ (MPa)	M (kg)	k (N/m)	f (Hz)
Triangular Silica	0	0	1.9	4.5	0.2	537.4	82.34
	75.5	3.57	–	0	–	–	–
Square Silica	0	0	3.4	7.94	0.35	806.1	75.8
	75.5	4.21	–	0	–	–	–

Table 2: *This table shows, based on the parameters in table 1 and the recorded deflection of each spring blade, the average values for the triangular and square silica spring blade. Notice the fiber stress goes to 0 when x is equal to L, this is because x is being observed from the very end of the blade.*

Table 2 shows the average results for the triangular and square spring blades. The values that are most important to this project is the breaking deflection, the fiber stress, and the mass at which the blade will break while holding. The stiffness is also worth noting because it shows how much the spring is able to bend. The frequency is also important because this is what will determine the noise level that silica or silicon can give off in future experiments to see if it is better than maraging steel for suspension systems. It can be noted that in table 2 the square silica spring blade has a greater deflection and fiber stress than the triangular one meaning it is a better design for the values that are sought out.

Spring Blade	x (mm)	y (mm)	P (N)	σ (MPa)	M (kg)	k (N/m)	f (Hz)
Blade 1	0	0	0.149	35.7	0.015	116.7	138.5
.	50	1.275	–	0	–	–	–
Blade 2	0	0	0.78	74.9	0.079	202.5	79.7
.	60	3.85	–	0	–	–	–
Blade 3	0	0	1.51	108.9	0.152	270.1	66.1
.	60	5.6	–	0	–	–	–
Blade 4	0	0	1.05	88.6	0.106	170.1	62.8
.	70	6.2	–	0	–	–	–
Blade 5	0	0	0.872	83.7	0.088	113.9	56.5
.	80	7.65	–	0	–	–	–

Table 3: *This table shows, based on the parameters in table 1 and the recorded deflection of each spring blade, the average values for the silicon spring blades.*

Table 3 shows the average results for the five silicon spring blades. The deflection, fiber stress, and mass should all be observed. Based off of these calculations and recording of the maximum deflection, the spring blade that is most fit to be used in a suspension system like the AEI prototype is blade 3 in table 3. This is because it is the only blade that can hold over 100 g with some room to make sure it doesn't hold too much and break. It is also the blade with the closest fiber stress that is to be expected from a silicon spring blade as we were aiming for 100-120 MPa.

The breaking patterns of each spring blade were very interesting when observed and are shown in figure 20. The triangular flamed silica spring blade broken where the flame polished surface met the un-flame polished surface very quickly due to the large change in strength. The square and triangular silica spring blades all broke closer to the fixed clamp. The smaller silicon blades, such as blade 1 and the extras, broke from both the free and fixed ends of the clamp. The larger silicon blades, such as blades 2-5, all exploded but the start of the breaking can be traced back to the left (fixed side of the clamp) middle.

breaks.jpeg 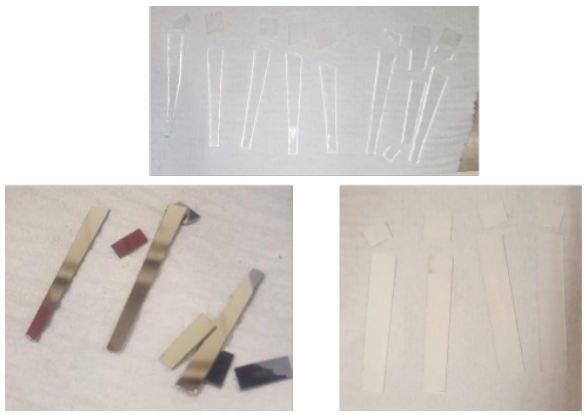

Figure 20: *Figure 20 shows breaking patterns for the triangular flame silica spring blades shown on the top, the smaller silicon spring blades shown in the bottom left, and the square silica spring blades that had the same pattern as the triangular spring blades. The larger silicon springs turned into piles of silicon but looked wonderful breaking on the high speed camera.*

Some sources of error in the experiment is the reading of the ruler off of the high speed camera video, varying placement of spring blades on clamp, uneven flame polishing, and uneven dremelling. The experiment was still accurate. The outliers laid with the triangular flamed silica spring blades, but they were left out of the data due to the improper flame polished surface causing them to fault. These errors could be fixed by getting a clearer picture on the camera, marking the spring blade ends when clamping them to know where they were clamped, and evenly flame polish and dremel the spring blades.

VI. Conclusion

The results yielded from the experiment were that the silicon blade 3 and square fused silica were the types of each spring blade material that were best "fitted" to go into a suspension system. Tables 2 and 3 show this claim through the higher fiber stress, mass held, and frequency. The issue with using either of these two spring blades is that the dimensions are not practical for the current AEI prototype. The spring blades are too larger to be put in and tested out but the fact remains that the materials can be useful spring blades in general.

The way that this problem could be fixed is to make more spring blades of differing values to get the fiber stress and mass held higher, with a lower frequency, and have different parameters so it is more likely to be placed into a suspension system.

Future work in silicon and fused silica springs will be taking place. Like it was mentioned in the last paragraph, if the parameters of either type of blade is manipulated and tested the right way, or perhaps specifically made to hold a 100g mass (so it can go into the AEI prototype). This is something that can be done to get a different material of spring blade into an actual suspension system. Another few things that could be done is changing the surface of these springs through a coating, etching, or giving it edge treatments. In the case of fused silica, there could be even more metal replaced in the AEI prototype because the spring blade could be fused silica and have a silica fiber melded to the spring blade to hand the test masses.

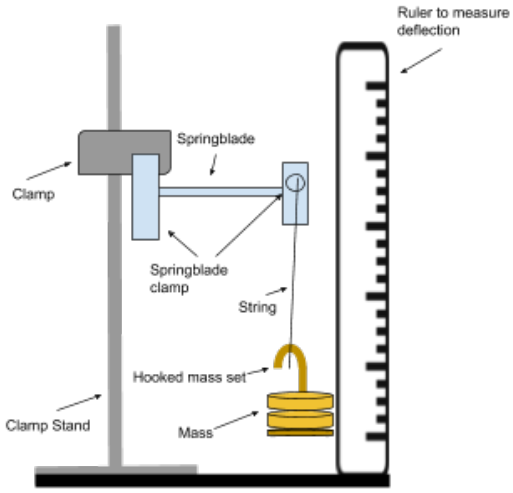

set set up.jpeg

Figure 21: *Figure 21 shows the layout of an experiment to test a spring blade's frequency.*

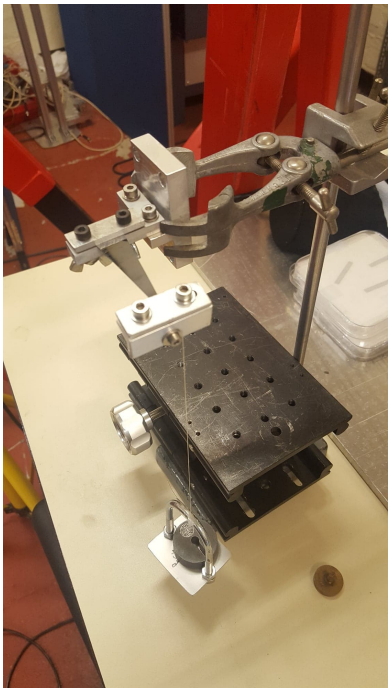

set up pic.jpeg

Figure 22: *Figure 22 was the set up of the experiment to test the spring blade's frequency. The blade being tested in this photo was silicon blade 3 and it was able to hold 107g (to give it a reasonable amount of room before it hits maximum weight, and because it corresponds with the weight held be the AEI prototype). The vibration set on it was recorded with the high speed camera and the video can be observed to find the frequency from there.*

Some more practical future work includes figuring out how many times a spring blade can be put to just under the maximum deflection point with a vertical load, brought back to zero deflection, and back to maximum

deflection, to see how this affects its strength. One experiment that could follow this one is shown in figure 21. The experiment was set up, shown in figure however due to time the frequencies were not able to be calculated from the high speed camera due to time restraints. Lastly, a tension load cell can be added to the spring breaking apparatus to measure the exact force at which the string is pulling on the spring blade. Also, taking a look at figure 12, as a vertical load is lowered onto the free end of the spring, it curves downwards. That is why the steel is originally made curved so when the load is added to the free end it lays flat. There isn't a way so far that fused silica or silicon can be bent in this fashion first or it will break. However, starting with a flat spring blade and suspending the weight on it will bend the spring blade. This is a challenge that can be faced by creating an apparatus that will rotate the bent spring blade so that the suspension becomes flat just like metal, but can stay still actually be bent like silicon or fused silica would be.

The low percent error for this experiment coupled with a few spring blades that look promising for future work and hopes for diving deeper into this project, it is quite accurate and a successful first shot at silicon and fused silica spring blades in suspension systems. More testing will confirm if there is a spring blade with the correct parameters to be put to use in an actual suspension system.

VII. Aknowledments

I am extremely grateful for the opportunity to participate in this international research experience funded by the National Science Foundation. Thank you to my mentors Dr. Giles Hammond and Dr. Alan Cumming who provided daily support and advice through out my research. Thank you to Mr. Karl Toland who helped me construct the spring breaking apparatus and all of the help given. Thank you to Mr. Colin Craig and Mr. Russel Jones for machining and designing parts for the spring breaking apparatus and silicon spring blades, respectively. Thank you to the program coordinators at the University of Florida: Dr. Guido Mueller, Dr.Bernard Whiting, Ms. Kristin Nichola, and Mr. Andrew Miller. Thank you to my advisor and wonderful professor at Moravian College, Dr. Ruth Malenda, for all of her help, support, and advice throughout my first research experience. I would like to thank everyone within the IGR and Physics department at University of Glasgow for being so welcoming.

VIII. References

[1] Albert Einstein. Naherungsweise Integration der Feldgleichungen der Gravitation, pages 99 108. Wiley-VCH Verlag GmbH Co. KGaA, 1916. ISBN 9783527608959. doi: 10.1002/ 3527608958.ch7. URL http://dx.doi.org/10.1002/3527608958.ch7.

[2] James Overduin. Special general relativity questions and answers what is a space time continuum?, 2010. URL https://einstein.stanford.edu/content/relativity/q411.html.

[3] R. M. Shannon, V. Ravi, L. T. Lentati, P. D. Lasky, G. Hobbs, M. Kerr, R. N. Manchester, W. A. Coles, Y. Levin, M. Bailes, N. D. R. Bhat, S. Burke-Spolaor, S. Dai, M. J. Keith, S. OsÂŁowski, D. J. Reardon, W. van Straten, L. Toomey, J.-B. Wang, L. Wen, J. S. B. Wyithe, and X.-J. Zhu. Gravitational waves from binary supermassive black holes missing in pulsar observations. Science, 349(6255):15221525, 2015. ISSN 0036-8075. doi: 10.1126/science.aab1910. URL http://science.sciencemag.org/content/349/6255/1522.

[4] S Gobler, A Bertolini, M Born, Y Chen, K Dahl, D Gering, C Graf, G Heinzel, S Hild, F Kawazoe, Kranz1,GKuhn ĬĹ , H Luck , K Mossavi, R Schnabel, K Somiya, K A Strain, J R Taylor, A Wanner, T Westphal, B Willke and K Danzmann. The AEI 10m prototype interferometer. IOP Science 2010 Class. Quantum Grav. 27 084023. URL http://iopscience.iop.org/0264-9381/27/8/084023. Web.

[5] Jones, Russell. (2012, August 12). AEI 10m prototype Suspensions: Lower suspension Blade (AEI-SUS-0005). Institute for Gravitational Research, University of Glasgow, Glasgow.

[6] Jones, Russell. (2012, August 12). AEI 10m prototype Suspensions: Upper suspension Blade (AEI-SUS-0004). Institute for Gravitational Research, University of Glasgow, Glasgow.

[7] Jones, Russell. (2018, July 2). Silicon Spring Blade Design 1. Institute for Gravitational Research, University of Glasgow, Glasgow.

[8] Jones, Russell. (2018, July 2). Silicon Spring Blade Design 2. Institute for Gravitational Research, University of Glasgow, Glasgow.

[9] Barclay, Sheena. Breaking Stress Measurements of Sapphire Springs. Institute for Gravitational Research, SUPA, University of Glasgow, Glasgow.

[10] Berkely. Deflection of Beams by Integration. http://www.me.berkeley.edu/ lwlin/me128/BeamDeflection.pdf.

[11] AZO materials. (2018). Silicon. https://www.azom.com/properties.aspx?ArticleID=1387

[12] AZO materials. (2018). Silica- Fused Silica. https://www.azom.com/properties.aspx?ArticleID=599

[13] Vitruvis. (2018). Normal Stress, Bending Stress, and Shear Stress. http://www.strucalc.com/normal-stress-bending-stress-shear-stress/

IX. Appendices

Appendix A:

Spring Blade	x (mm)	Actual y (mm)	y (mm)	σ (MPa)	k (N/m)	f (Hz)	% difference of y
Lower Blade	0	0	0	654	3.78	9.66	–
	55	27.1	26	0	–	–	2.41
Upper Blade	0	0	0	461.1	6.56	8.75	–
	65	32.63	32	0	–	–	3.21

Table 4: *This table shows, based on the parameters in figures 2 and 3, the calculations for maraging steel in the AEI prototype at Glasgow. It also shows the percent different of deflection found in the model and deflection found using the equation 6. It shows that the mathematical equation is accurate to determine deflection from the low percent differences,*

The predictive calculations for the upper and lower spring blades made of maraging steel are shown in table 4. The low percent difference of the lower blade and upper blade of 2.41% and 3.21 % show that the equation used is accurate to depict the deflection.

Appendix B

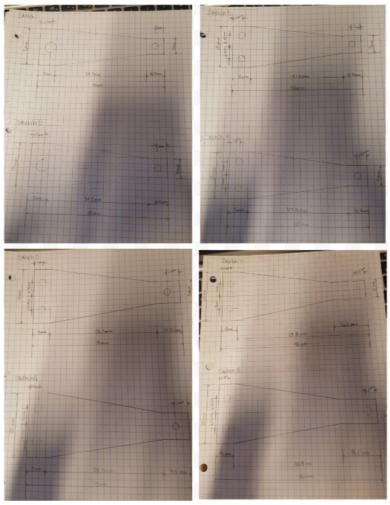

Figure 23: *Figure 23 shows the sketches that were originally designed for the silicon spring blades. The designs ended up being narrowed down as well as the holes removed because the clamp used in the spring breaking apparatus is flat and without screws so the design did not have to directly follow that of the maraging steel blades in the AEI suspension. Also, at this point in the experimental process for silicon blades it was not yet necessary. These designs were modelled in CAD and are shown in figures 5 and 6 to be laser cut and experimented on.*

.

Appendix C: The triangular flamed spring blade's data, figures 24 and 25 and, and averages, show that there

was an error in its conception. The unevenness of the flame polishing coupled with the whole blade not being flame polished gave results that were not accurate or followed any prediction of the flame polished blade being strong than an unpolished fused silica spring blade.

fl deflection.jpeg

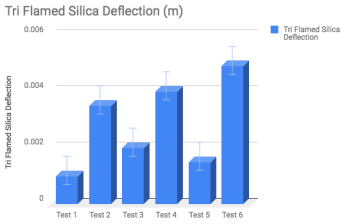

Figure 24: *Figure 24 shows the individual data for the deflection of the triangular flamed silica spring blades. The horizontal axis shows each test with a 0.5mm error bar for reading the camera, and the vertical axis is in meters. As noticed, these results were all over the place and only test 6 shows how strong the flame polished blades should be as I clamped it further down the polished surface rather than at the unpolished tip that cause it to break from the difference in surfaces.*

flame stress.jpeg

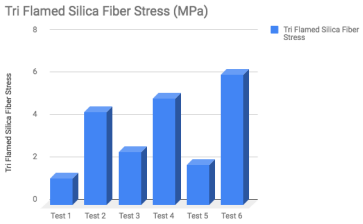

Figure 25: *Figure 25 shows the individual data for the fiber stress of the triangular flamed silica spring blades. The horizontal axis shows each test and the vertical axis is in MPa. As noticed, these results were all over the place following suit with the deflection.*